

Experimental study of the spin-orbit quantum interference effect in a high-mobility $\text{In}_x\text{Ga}_{1-x}\text{As}/\text{InP}$ quantum well structure with strong spin-orbit interaction

G. Yu, N. Dai, and J. H. Chu

National Laboratory for Infrared Physics, Shanghai Institute of Technical Physics, Chinese Academy of Science, Shanghai 200083, People's Republic of China

P. J. Poole and S. A. Studenikin*

Institute for Microstructural Sciences, National Research Council of Canada, Ottawa, Ontario K1A 0R6, Canada

(Received 2 January 2008; published 1 July 2008)

The quantum interference corrections to magnetoconductivity were studied experimentally in a gated high-mobility $\text{In}_x\text{Ga}_{1-x}\text{As}/\text{InP}$ quantum well structure with strong spin-orbit interaction. The phase-breaking time and spin splitting were extracted by fitting the experimental data using a recent model [L. E. Golub, *Phys. Rev. B* **71**, 235310 (2005)], which is applicable to arbitrarily strong spin-orbit coupling and magnetic field. It is experimentally verified that this model satisfactorily describes the data over a large range of magnetic fields extended from diffusion to nondiffusion regimes. The obtained dependencies of the phase-breaking and spin-relaxation time constants vs temperature and the gate voltage are in good agreement with existing theoretical predictions.

DOI: [10.1103/PhysRevB.78.035304](https://doi.org/10.1103/PhysRevB.78.035304)

PACS number(s): 73.20.Fz, 72.25.Rb, 73.63.Hs, 85.75.-d

I. INTRODUCTION

The weak antilocalization (WAL) effect has often been exploited to investigate the zero-field spin splitting¹⁻⁹ due to spin-orbit (SO) interaction. The arising correction to the conductivity as a function of small magnetic field has a non-monotonic dependence with a minimum, whose position is directly related to the spin splitting at zero magnetic field. The SO coupling forms the basis of various proposals for spintronic devices including spin qubits for quantum computing implementations.¹⁰⁻¹²

There are two main SO interaction mechanisms leading to the spin splitting at zero magnetic field. The first mechanism is due to a lack of crystal inversion symmetry resulting in linear and cubic Dresselhaus terms.¹³ The second mechanism arises from structural macroscopic asymmetry due to an electric field present in a quantum well. The latter mechanism, commonly referred as the Rashba effect, is more appealing in the sense of potential practical applications as it enables us to control electronic spin states by gate voltages, which can be made much faster and spatially smaller as compared to the magnetic-field techniques.^{4-7,14}

Most of the works on SO interaction using the WAL phenomenon were performed on samples with relatively low electron mobility and small SO coupling. On the other hand, for spin-electronic applications, such as quantum circuits, it is necessary to use high-mobility structures and, therefore, to develop proper methods to characterize their SO properties for further device engineering.^{5-7,9} Much less work has been done on high-mobility samples with strong SO coupling. To extract SO coupling and phase-breaking time from the interference corrections to magnetoresistance, it is common to use the analytical equations derived in the so-called diffusion regime by Hikami, Larkin, and Nagaoka (HLN),¹ and by Iordanskii *et al.*,³ which are both valid only for small magnetic fields and small SO interaction. Experimental study of the WAL effect in high-mobility $\text{In}_x\text{Ga}_{1-x}\text{As}/\text{InP}$ quantum

wells^{6,7} revealed that neither of these theories could adequately fit the experimental results in the whole range of magnetic field studied. For example, in Ref. 6 an empirical factor of 2 had to be introduced in order to satisfactorily fit the data. It was obvious that the existing models failed to describe the experimental dependencies when the conditions of small magnetic field and small SO coupling were not satisfied.

There is a model of the WAL effect for the limit of high magnetic fields,⁵ but it is not suitable for small magnetic fields and, therefore, is not applicable to describe experimental data in the whole range of magnetic field. Only recently, an analytical theory was developed by Golub⁸ beyond the diffusion approximation to assess such a situation of both small and strong ranges of magnetic field and SO coupling. This model has not yet been tested experimentally on an appropriate set of experimental data with a well-developed WAL minimum.

In this paper we experimentally verify the validity of the model⁸ to describe the interference corrections to the conductivity in a high-mobility $\text{In}_x\text{Ga}_{1-x}\text{As}/\text{InP}$ sample with strong SO coupling. We find that experimental data can be well fitted using this theoretical model over a large range of magnetic fields from small to high beyond the diffusion limit. The phase-breaking time (τ_ϕ) dependence as a function of temperature and the gate voltage agrees well with the theoretical predictions. The product $\Omega\tau$ is found to be larger than unity, whereas the spin-split energy due to SO coupling is comparable to that observed in lower mobility samples and follows the expected square-root dependence against electron density ($\Delta_R = 2\alpha k_f = 2\hbar\Omega$).

II. THEORETICAL EQUATIONS AND FITTING PROCEDURE

The diffusion regime is usually reached in low-mobility structures, which requires the following two conditions to be

satisfied: (1) the strength of SO interaction is small: $\Omega\tau \ll 1$, and (2) magnetic field intensity is small, too, in terms of $B \ll B_{tr} = \hbar/(2el^2)$, where B_{tr} is the ‘‘transport’’ magnetic field, e is the electronic charge, and l is the mean free path. The HLN¹ and Iordanskii *et al.*³ models are applicable to describe experimental data in this situation.⁹ In high-mobility samples, like in our case, the product $(\Omega\tau)$ becomes comparable to or larger than unity or, equivalently, the SO precession length becomes shorter than the electron mean free path. In addition, in high-mobility samples the transport field B_{tr} often becomes less than 1 mT and both the above conditions fail. Therefore, HLN and Iordanskii’s models cannot be employed to describe the WAL effect in high-mobility samples with strong SO coupling.

Below we present equations for the WAL effect following Golub’s work⁸ and the fitting procedure to extract the SO and phase-relaxation parameters. In the case when only one of the SO mechanisms is dominant,¹⁵ i.e., Rashba or Dresselhaus mechanism, the expression for the WAL corrections to conductivity in arbitrary strong magnetic field can be presented in the following form:

$$\sigma(B) = \sigma_a(B) + \sigma_b(B), \quad (1)$$

where σ_a and σ_b can be interpreted as respective contributions due to the backscattering and nonbackscattering interference corrections to the conductivity:

$$\sigma_a = -\frac{e^2}{2\pi^2\hbar} \left(\frac{l}{l_B}\right)^2 \sum_0^\infty \left\{ \text{Tr}[A_N^3(I - A_N)^{-1}] - \frac{P_N^3}{1 - P_N} \right\}, \quad (2)$$

$$\begin{aligned} \sigma_b = & \frac{e^2}{4\pi^2\hbar} \left(\frac{l}{l_B}\right)^2 \sum_0^\infty \left\{ \text{Tr}[K_N \tilde{K}_N A_N (1 - A_N)^{-1}] \right. \\ & + \text{Tr}[\tilde{K}_N K_N A_{N+1} (1 - A_{N+1})^{-1}] \\ & \left. - Q_N^2 \left(\frac{P_N}{1 - P_N} + \frac{P_{N+1}}{1 - P_{N+1}} \right) \right\}. \end{aligned} \quad (3)$$

There are two contributions of the singlet and the triplet terms in both σ_a and σ_b . The matrix terms represent the triplet contribution, which has opposite sign to the singlet one. The matrix A_N is given by

$$A_N = \begin{pmatrix} P_{N-2} - S_{N-2}^{(0)} & -R_{N-2}^{(1)} & S_{N-2}^{(2)} \\ R_{N-2}^{(1)} & P_{N-1} - 2S_{N-1}^{(0)} & -R_{N-1}^{(1)} \\ S_{N-2}^{(2)} & R_{N-1}^{(1)} & P_N - S_N^{(0)} \end{pmatrix}, \quad (4)$$

where

$$P_N = \frac{l_B}{l} \int dx \exp\left(-x \frac{l_B}{\tilde{l}} - \frac{x^2}{2}\right) L_N(x^2),$$

$$\begin{aligned} S_N^{(m)} = & \frac{l_B}{l} \sqrt{\frac{N!}{(N+m)!}} \int_0^\infty dx \\ & \times \exp\left(-x \frac{l_B}{\tilde{l}} - \frac{x^2}{2}\right) x^m L_N^m(x^2) \sin^2\left(\Omega \tau \frac{l_B}{l} x\right), \end{aligned}$$

and

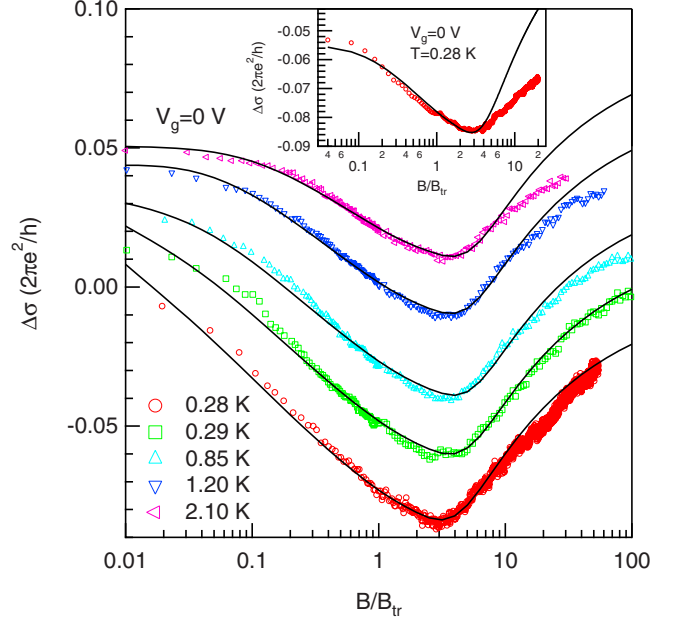


FIG. 1. (Color online) Experimental magnetoresistance traces $\Delta(1/\rho) = 1/\rho_{xx} - 1/\rho_0$ (symbols) for different temperatures, along with the theoretical fits (solid curves) by Eq. (1) using two fitting parameters. The inset shows an experimental magnetoconductance $\Delta(1/\rho) = 1/\rho_{xx} - 1/\rho_0$ (symbols) for $T=0.28$ K and $V_g=0$ V, along with the two parameter fits by the HLN model (Ref. 1) (solid line).

$$\begin{aligned} R_N^{(m)} = & \frac{l_B}{l\sqrt{2}} \sqrt{\frac{N!}{(N+m)!}} \int_0^\infty dx \\ & \times \exp\left(-x \frac{l_B}{\tilde{l}} - \frac{x^2}{2}\right) x^m L_N^m(x^2) \sin\left(2\Omega \tau \frac{l_B}{l} x\right). \end{aligned}$$

where $\tilde{l} = l/(1 + \tau/\tau_\phi)$ is the effective scattering length.

$$K_N = \begin{pmatrix} Q_{N-2} - S_{N-2}^{(1)} & R_{N-2}^{(2)} & S_{N-2}^{(3)} \\ -R_{N-1}^{(0)} & Q_{N-1} - 2S_{N-1}^{(1)} & R_{N-1}^{(2)} \\ -S_{N-1}^{(1)} & -R_N^{(0)} & Q_N - S_N^{(1)} \end{pmatrix}. \quad (5)$$

$$\tilde{K}_N = \begin{pmatrix} Q_{N-2} - S_{N-2}^{(1)} & -R_{N-1}^{(0)} & -S_{N-1}^{(1)} \\ R_{N-2}^{(2)} & Q_{N-1} - 2S_{N-1}^{(1)} & -R_N^{(0)} \\ S_{N-2}^{(3)} & R_{N-1}^{(2)} & Q_N - S_N^{(1)} \end{pmatrix}. \quad (6)$$

$$Q_N = \frac{1}{\sqrt{N+1}} \frac{l_B}{l} \int dx \exp\left(-x \frac{l_B}{\tilde{l}} - \frac{x^2}{2}\right) x L_N^1(x^2).$$

In the fitting procedure the summation for both σ_a and σ_b had to be performed up to large numbers of N up to $\sim 200\,000$ because the convergence was very slow, in particular, in low magnetic fields. The computed function $\sigma(B, \tau/\tau_\phi, \Omega\tau) = \sigma_a(B, \tau/\tau_\phi, \Omega\tau) + \sigma_b(B, \tau/\tau_\phi, \Omega\tau)$ was stored numerically as a matrix on a semilogarithmic mesh. Intermediate values between neighboring points $(B_i, \tau/\tau_{\phi i}, \Omega\tau_i)$ and $(B_{i+1}, \tau/\tau_{\phi i+1}, \Omega\tau_{i+1})$ were determined by spline interpolation.

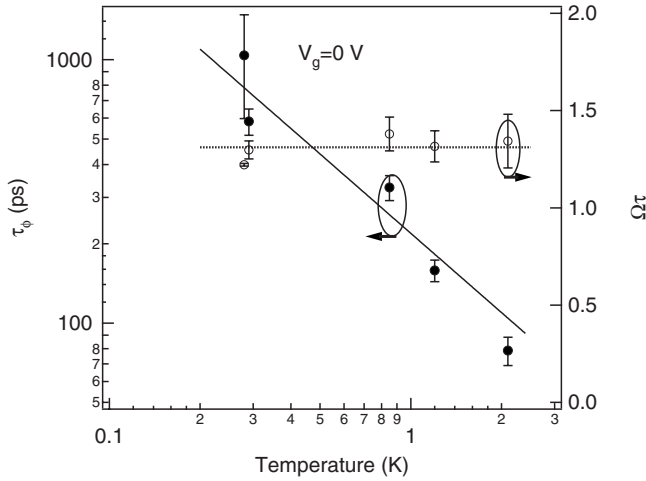


FIG. 2. Phase-breaking time τ_ϕ (solid circles) and $\Omega\tau$ (open circles) extracted by fitting experimental data in Fig. 1 as a function of temperature. The solid line is a theoretical limit due to the electron-electron scattering by Eq. (7). The dashed line indicates a mean value of $\Omega\tau$.

III. EXPERIMENT

The gated Hall bar sample studied in this work was fabricated from a high-mobility $\text{In}_x\text{Ga}_{1-x}\text{As}$ quantum well structure grown by chemical beam epitaxy on an InP (100) substrate.⁶ This sample was of particular interest because it exhibited large SO effects, so the parameter $\Omega\tau > 1$, where Ω is the cyclic SO precession frequency, and τ is the transport scattering time constant. The quantum well is formed by a 10-nm layer of $\text{In}_x\text{Ga}_{1-x}\text{As}$ ($x=0.53$) grown on an undoped InP buffer layer and separated from the Si-doped region by a 30-nm spacer. A rectangular Hall bar sample, with a width of 0.2 mm and a separation between adjacent potential probes of 0.4 mm, was fabricated using standard optical lithography and wet etching. A gold gate was deposited on top of a 40-nm SiO_2 dielectric layer. Experiments were performed in an Oxford ^3He cryostat equipped with a superconducting solenoid.

The experimental values of the interference correction $\Delta\sigma$ were calculated as $(1/\rho_{xx}) - (1/\rho_0)$, which classically do not have any field dependence. Temperature dependence of the longitudinal magnetoconductance is shown in Fig. 1. The solid lines are the fits by Eq. (1) with two dimensionless fitting parameters τ/τ_ϕ and $\Omega\tau$. The parameter B_{tr} has a constant value at each temperature and gate voltage and is determined from independently measured values of electron density and mobility shown in the inset of Fig. 3. In this figure, except for the curve at $T=0.28$ K, all curves are shifted vertically for clarity. It is evident from the figure that the theory describes the experiment very well up to unprecedented high values of relative magnetic fields reaching $B/B_{tr} \sim 50$, which was impossible with earlier theoretical models.^{6,7} Even by itself, this is a very important result. It is an experimental verification of the model⁸ to describe the WAL effect in samples with strong SO interaction in the whole range of arbitrarily strong magnetic field.¹⁶

The inset in Fig. 1 shows an example of the WAL effect fitted with the HLN equation¹ (solid line). The best fit pa-

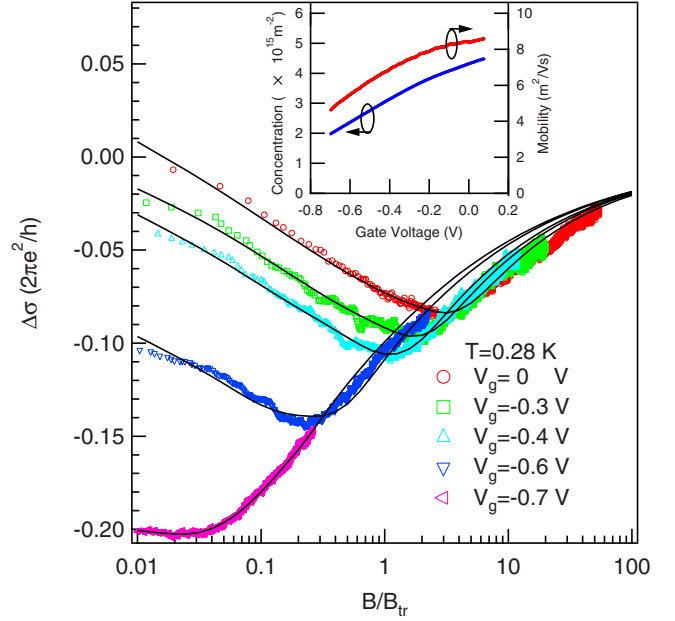


FIG. 3. (Color online) Experimental magnetoconductance $\Delta(1/\rho) = 1/\rho_{xx} - 1/\rho_0$ (symbols) for several gate voltages at $T = 0.28$ K, along with the two parameter fits by Eq. (1) (solid curves). The inset shows electron concentration and mobility dependencies vs gate voltage.

rameters are the following: $\tau_\phi = 1.04$ ns, $\Omega\tau = 1.22$ (using Golub's model⁸), and $\tau_\phi = 5.1$ ns, $\Omega\tau = 0.37$ (using HLN¹). It is evident that the HLN equation fails to describe the experiment due to the reasons discussed above. In addition, a large error may occur in determined values of τ_ϕ and the SO constant if improper equations are used. In other words, it is important to use adequate theoretical equations to extract SO characteristics of two-dimensional electrons. It should be noted that in order to determine SO coupling in high-mobility samples, it is necessary to perform measurements and fitting up to high magnetic fields because the WAL minimum occurs in a high-field region ($B/B_{tr} > 1$).

IV. DISCUSSION

Figure 2 shows the phase-breaking time τ_ϕ and $\Omega\tau$ as a function of temperature extracted from the data in Fig. 1. Experimental values for τ_ϕ coincide well with the theoretical prediction (solid line) based on a Fermi-liquid model involving small energy transfer at each inelastic electron-electron scattering event:²

$$\frac{1}{\tau_\phi} = \frac{k_B T \pi G_0}{\hbar \sigma_0} \ln\left(\frac{\sigma_0}{2\pi G_0}\right), \quad (7)$$

where $G_0 = e^2(\pi\hbar)$. This model is valid for $k_B T \tau / \hbar \ll 1$, which is applicable to our case of electron mobilities ≈ 50000 cm^2/Vs and $T \leq 2$ K. Theoretically, according to the D'yakonov-Perel' spin-dephasing mechanism,¹³ the SO parameter $\Omega\tau$ is a constant, which does not depend on temperature.¹⁷ This supports our observation in Fig. 2. The average value of $\Omega\tau = 1.31$ is indicated by the dashed line,

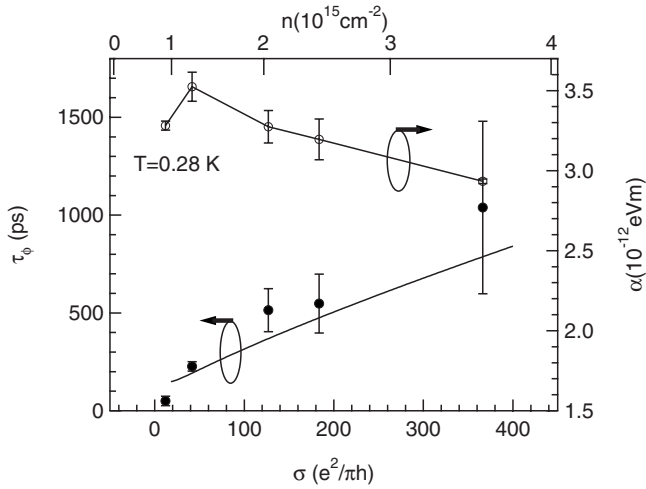


FIG. 4. Phase-breaking time τ_ϕ (solid circles) and spin-orbit constant α (open circles) extracted by fitting data in Fig. 3 as a function of the gate voltage. The solid line is a theoretical limit for τ_ϕ by Eq. (7).

which will be used in Fig. 3 as one point at a temperature of 0.28 K.

The magnetoconductivity dependence at $T=0.28 \text{ K}$ for different gate voltages is shown in Fig. 3. In this figure all experimental curves are shifted vertically to coincide with their corresponding theoretical ones, which represent the absolute magnitudes of the conductivity corrections due to weak localization. Again, excellent agreement between measurements and calculated curves is obtained in the whole range of magnetic fields up to $B/B_{\text{tr}} \sim 100$. The WAL minimum position shifts toward higher values of B/B_{tr} for higher gate voltages, which correspond to higher electron densities. Note that B_{tr} is a function of electron concentration and mobility and can be estimated from the inset in Fig. 3 using the following practical equation: $B_{\text{tr}} = 0.121/(n\mu^2)$, where B_{tr} is in Tesla, n is electron concentration in 10^{15} m^{-2} , and μ is mobility in m^2/Vs .

The results obtained from fitting the data in Fig. 3 are plotted in Fig. 4 as a function of two-dimensional electron gas (2DEG) conductivity. The phase-breaking time is in agreement with the Fermi-liquid model Eq. (7) within an experimental uncertainty for this parameter. The uncertainty is larger for larger electron concentrations. The uncertainty increases because the WAL maximum at $B=0$ becomes very narrow for higher electron mobility, and only a few points become available within the $B=0$ WAL peak for fitting.

The dependence of SO parameter α vs electron concentration (top scale in Fig. 4) agrees well with the results in Ref. 7 obtained in different experiment on this sample. In current work, though, the study is extended to smaller range of electron concentrations. At smaller electron concentration we find that the SO constant has a nonmonotonous dependence with a maximum of $3.5 \times 10^{-12} \text{ eV/m}$ at $n \approx 1.2$

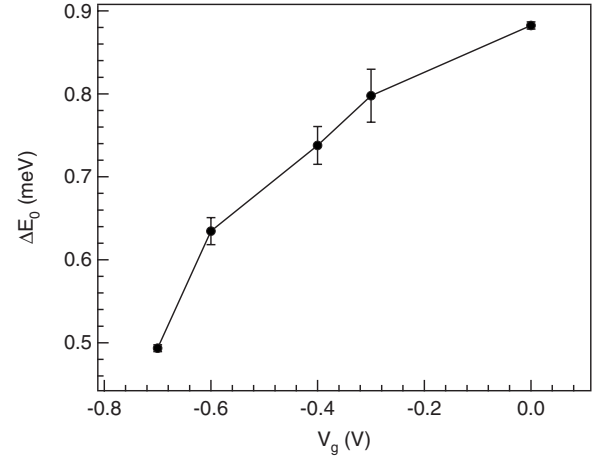


FIG. 5. Calculated spin-splitting energy at zero magnetic field vs gate voltage.

$\times 10^{15} \text{ m}^{-2}$. A similar nonmonotonous dependence of SO constant was observed earlier in a strained InGaAs/InP quantum well structure,¹⁸ which could not be understood as an interplay between Rashba and Dresselhaus terms vs gate voltage. This nontrivial behavior of the SO constant still awaits its explanation.

Let us now estimate the spin-splitting energy $\Delta E_0 = 2\hbar\Omega$ (Ref. 8) using results for α in Fig. 4. The Rashba SO constant can be calculated using the following relation $\Delta E_0 = 2\hbar\Omega = 2\alpha k_F$, with $k_F = \sqrt{2\pi n}$ being the electron Fermi wave vector. Although the overall change of the SO parameter in Fig. 4 is not very large, variation of the spin-split energy is much bigger due to its dependence on the Fermi momentum. Figure 5 shows the spin-split energy at zero magnetic field vs gate voltage. It is evident from the figure that we are able to change the spin splitting in this sample between 0.5 and 1 meV by varying gate voltage between -0.7 and 0 V.

V. CONCLUSIONS

In conclusion, the weak antilocalization effect in a high-mobility InGaAs/InP quantum well structure with strong spin-orbit coupling was investigated experimentally to verify the recently developed universal model⁸ for arbitrary strengths of spin-orbit coupling and magnetic field. It is demonstrated that this model is applicable to describe the experimental data over a large range of magnetic fields continuously within and beyond the diffusion limit. It is important to use an adequate model to extract exact values of spin-orbit characteristics.

ACKNOWLEDGMENTS

This work was supported in part by the Knowledge Innovation Program of the Chinese Academy of Sciences (C2-12), and the Special Funds for Major State Basic Research under Project No. 2007CB924900.

*Corresponding author: sergei.studenikin@nrc.ca

- ¹S. Hikami, A. I. Larkin, and Y. Nagaoka, *Prog. Theor. Phys.* **63**, 707 (1980).
- ²B. L. Altshuler, A. G. Aronov, and D. E. Khmel'nitzkii, *J. Phys. C* **15**, 7367 (1982).
- ³S. V. Iordanskii, Yu. B. Lyanda-Geller, and G. E. Pikus, *JETP Lett.* **60**, 206 (1994).
- ⁴T. Koga, J. Nitta, T. Akazaki, and H. Takayanagi, *Phys. Rev. Lett.* **89**, 046801 (2002).
- ⁵J. B. Miller, D. M. Zumbuhl, C. M. Marcus, Y. B. Lyanda-Geller, D. Goldhaber-Gordon, K. Campman, and A. C. Gossard, *Phys. Rev. Lett.* **90**, 076807 (2003).
- ⁶S. A. Studenikin, P. T. Coleridge, N. Ahmed, P. J. Poole, and A. Sachrajda, *Phys. Rev. B* **68**, 035317 (2003).
- ⁷S. A. Studenikin, P. T. Coleridge, G. Yu, and P. J. Poole, *Semicond. Sci. Technol.* **20**, 1103 (2005).
- ⁸L. E. Golub, *Phys. Rev. B* **71**, 235310 (2005).
- ⁹B. Grbić, R. Leturcq, T. Ihn, K. Ensslin, D. Reuter, and A. D. Wieck, *Phys. Rev. B* **77**, 125312 (2008).
- ¹⁰S. A. Wolf, D. D. Awschalom, R. A. Buhrman, J. M. Daughton, S. von Molnar, M. L. Roukes, A. Y. Chtchelkanova, and D. M. Treger, *Science* **294**, 1488 (2001).
- ¹¹V. Cerletti, W. A. Coish, O. Gywat, and D. Loss, *Nanotechnology* **16**, R27 (2005).
- ¹²M. A. Kastner, *Proc. IEEE* **93**, 1765 (2005).
- ¹³P. D. Dresselhaus, C. M. A. Papavassiliou, R. G. Wheeler, and R. N. Sacks, *Phys. Rev. Lett.* **68**, 106 (1992).
- ¹⁴M. Governale, D. Boese, U. Zülicke, and C. Schroll, *Phys. Rev. B* **65**, 140403(R) (2002).
- ¹⁵It is found that in InGaAs quantum well structures, the Rashba term often prevails (Refs. 4–7).
- ¹⁶During the preparation of this manuscript, a paper by Guzenko *et al.* (Ref. 19) has appeared where the authors use Golub's model (Ref. 8) to fit their data. However, only the WAL peak around $B=0$ was fitted in this paper because the WAL minimum was much less evident as compared to the present work; therefore, the validity issue in the whole range of magnetic fields could not be verified, and has not been discussed.
- ¹⁷The parameter $\Omega\tau$ equals to $\sqrt{\beta_{\text{SO}}}$, where $\beta_{\text{SO}}=\tau/\tau_{\text{SO}}$ was used in Ref. 6 as a fitting parameter.
- ¹⁸S. A. Studenikin, P. T. Coleridge, P. Poole, and A. Sachrajda, *JETP Lett.* **77**, 311 (2003).
- ¹⁹V. A. Guzenko, T. Schäper, and H. Hardtdegen, *Phys. Rev. B* **76**, 165301 (2007).